KIMYO INTERNATIONAL UNIVERSITY IN
CENTRAL ASIAN JOURNAL OF STEM
ISSN 2181-2934 http://stem.ytit.uz/

Investigations on Tribological Behavior and Wear Mechanisms of Inconel X-750 Alloy in Fretting Condition

Ibrohim Rustamov [a,b] and Zixi Wang [a]

[a]*State Key Laboratory of Tribology, Tsinghua University, Beijing 100084, China*

[b]*Department of Energy and Applied Sciences, Yeoju Technical Institute in Tashkent, Tashkent 100121, Uzbekistan*

Email: i.rustamov@ytit.uz; zxwang@tsinghua.edu.cn

Abstract

Fretting wear characteristics of Inconel X-750 were investigated under the dry test condition. Ball-on-flat contact configuration was subjected to the oscillatory movement of different sliding amplitudes through the different time duration and normal loading. Fretting tests were carried out on the high frequency wear test rig SRV 4 at room temperature with ~60% relative humidity. Wear evolutions and fretting damage mechanisms were analyzed in the case of partial slip (PS) and gross slip (GS) regimes in respect of displacement amplitude, normal load and time. Surface morphologies were investigated by 3D optical profiler, scanning electron microscopy (SEM) and energy dispersive spectroscopy (EDS). It is found that displacement amplitude and normal load had strong effect on the fretting mode and damage mechanism. Matter removal by abrasive wear was dominant under the lower loads while cracks induced by fatigue were observed for higher loads during PSR, and the wear mechanisms were transformed to the damage of debris oxidization and delamination at GSR. Fretting time dependence was critical in the higher displacement amplitudes where wear volume progressed significantly. However, test duration is less consistent in the partial slip regimes ($\leq$ 40 μm) where the wear rate and wear scar remain unchanged over time.

Keywords: Fretting, slip regimes, friction, wear evolution, damage mechanisms.

1. Introduction

Fretting refers to a complex phenomenon where two adjacent surfaces in a contact are subjected to a small amplitude relative oscillatory motion, often at high frequencies for a number of cycles. Fretting process is greatly affected by the tribological parameters (stroke length, normal load, frequency of motion and environmental factors), which cause different running conditions and material responses [1]. Vincent et al. [2] introduced the concept of fretting map in order to grasp the principles of material response in different slip regimes (Fig. 1). The evolution of sliding conditions can be identified by the formation of *"normal load – displacement amplitude"* diagram which is stick slip or partial slip regime (PSR) is defined by closed or elliptical loop and gross slip

regime (GSR) is characterized by open or quasi-rectangular cycles. Classical Mindlin`s elastic model describes these two fretting conditions depending on the imposed displacement [3]. If the displacement amplitude is small enough, the corresponding tangential load is less than the product of normal load related with total sliding. In this case, partial slip takes place where the contact is divided into two zones: a central stick zone and an external slip annulus. As the displacement amplitude increases, the tangential load reaches the critical total sliding value, thus the gross slip occupies the whole contact interface. Further increase in the displacement amplitude (often greater than the contact length) leads to the reciprocating sliding. Zhou and Vincent [4] also introduce the mixed fretting regime (MFR) which lays between partial slip and gross slip regimes. MFR was recognized the most critical regime in the fretting tests where the materials can fail due to overstraining and overstressing. In the consequence of partial and mixed slip regimes, surface damages can be fatigue cracks which is analyzed using the tools of fatigue failure and gross slip is mainly associated with debris formation or material removal which is investigated by considering energy dissipation in the contact [5]. The tendency of the contact to produce wear debris is higher in the lower normal loads and greater displacement amplitudes while the higher loads induce crack initiation and propagation. It is more proper to consider fretting wear as an oscillatory movement for which small displacements are a consequence of external vibration while fretting fatigue as a result of one of the mating surfaces being exposed to a cyclic stress, leading to cracking which is most damaging mechanism [6].

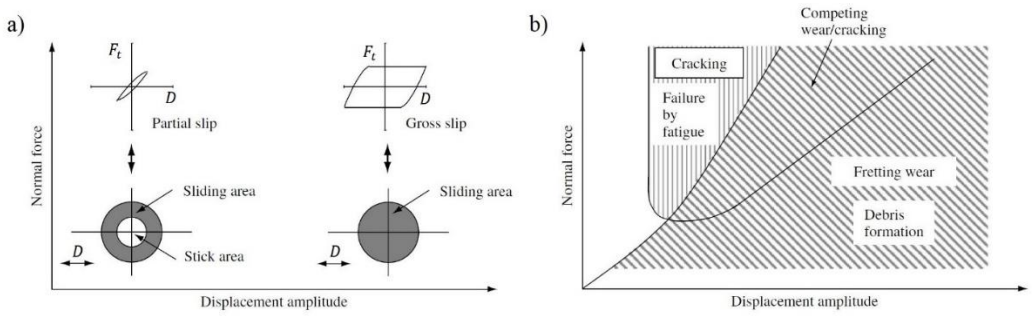

Fig. 1. (a) Partial slip and gross slip regimes in fretting for a ball-on-flat contact configuration [6]; (b) material response fretting map [5].

Moreover, several wear mechanisms induced by fretting were observed such as adhesive wear and plastic deformation in the onset of fretting, and oxidization and delamination wear damages during steady-state behavior. For metallic surfaces, the wear debris are trapped, crushed and oxidized in the contact interface which triggers the formation of reddish powder [7].

One of the most studied aspects of the fretting is to identify the demarcation line between fretting and reciprocating sliding wear. It is known that in the fretting process the wear coefficient rapidly increases as the amplitude of motion increases. On the other hand, reciprocating sliding wear volumes are kept constant as long as total sliding movements are consistent [8]. The displacement amplitude is mainly taken into consideration as an influencing factor of a transition from fretting to reciprocating sliding. And because of the complexity of the fretting process (including material type and contact conditions etc.), the ambiguity of the amplitude effect remains in the literatures. Thus, different transition values were reported, i.e., Toth [9] proposes peak-to-peak (twofold displacement amplitude) value of 50μm as a transition from fretting wear to reciprocating sliding while Lewis and Didsbury [10] and Vingsbo and Soderberg [11] suggest 70 μm and 300 μm, respectively.

The basics of fretting wear mechanisms is conveniently studied by experiments with the means of laboratory test rig using suitable contact configuration. The sphere-on-flat surface type is widely used among the scientists mainly due to the precise contact location and the alignment of the specimens interacts without mishap and they can be cheaply machined. As for the mating materials, many fretting wear tests were performed using homogeneous and inhomogeneous mating materials, in combination with ceramics [7,12], steel [13-15], alloys [4,16,17], polymers [18] and DLC/GLS coated materials [19,20].

In this study, the fretting wear experiments of Inconel X-750 alloy were carried out in ambient temperature and wear scars were analyzed in respect of normal load, displacement amplitude and time. The nickel-chromium super alloy Inconel X-750 is a precipitation-hardenable alloy which has been used in many applications such as gas turbines, jet engine parts, nuclear power plant applications, heat-treating fixtures, forming tools and springs or bolts [21]. It has the excellent mechanical properties and resistance to chemical corrosion and oxidation, as well as maintains good performance at temperatures up to 650℃. Inconel X-750 has been successfully applied to manufacture bump type gas foil bearings which operate at high-speed rotation and high temperature conditions. This type of bump and flat bearing foils make high concentrated line or point contacts and subjected to a small relative motion between each other in order to support a rotor on the other side. The fretting regime varies along the bearing angle and mostly dissipates the energy which is coming from the vibrating rotor [22]. Current process is mostly related to produce wear debris and fatigue cracking on the material under the high frequency stress cycles. No previous studies include the experimental fretting wear behaviors of Inconel X-750 alloy, therefore there is a need to perform more fretting wear experiments by analyzing its tribological response to such an operating regime to enhance its reliability.

2. Experiment

2.1 Specimens

Fretting wear tests were carried out in a high frequency SRV 4 Optimol (Germany) tribosystem with a ball-on-flat configuration. Fig. 2 shows the test chamber and the contact schematics of the frictional couples. The upper specimen was an oscillating GCr15 steel ball (GB 308-89, Chinese) with 10mm in diameter and roughness Ra of 2.0. The lower specimen was a stationary solution heat treated (annealed at 980℃) Inconel X-750 disk with the dimensions of height 7.5×diameter 24 mm. Young`s modulus and Poisson`s ratio was 210 GPa and 0.3 for GCr15, 214 GPa and 0.29 for the lower specimen, respectively. Table 1 lists the chemical compositions of the coupled materials. The micro harnesses of the materials were measured by micro-indenter *"Qness"* (Austria) tester with a pyramidal diamond tip (20 μm), 760 and 298 HV 0.3 were obtained for GCr15 ball and Inconel X-750 disk, respectively. Once the lower specimens were machined, top surfaces were ground subsequently using waterproof SiC paper with grain sizes of 15, 8 and 5 μm to gradually eliminate the abrasive asperity peaks. Then polished with 1μm water based polycrystalline diamond suspension to have a mirror finish. Specimens were ultrasonically cleaned with ethanol for 20 minutes and dried by compressed air blowing prior to the fretting tests.

Table 1. Chemical composition of Inconel X-750 alloy and GCr15 steel.

Materials	Elements										
	Ni	Cr	Fe	Ti	Al	Mn	Si	S	Cu	C	P
Inconel X-750	≥70	14-17	5-9	2.25-275	0.4-1	≤1	≤0.5	≤0.01	≤0.5	≤0.08	≤0.015
GCr15	≤0.3	1.4-1.65	Bal	-	-	0.25-0.45	0.15-0.35	≤0.025	≤0.25	0.95-1.05	≤0.025

2.2 Test conditions and analyses

Fretting wear tests were conducted in a room temperature (20-25℃) with a relative humidity of 55-65% in dry contact condition. Parameters were set under different normal load conditions, stroke length, frequency and test durations. Oscillating motions were kept under 50 N and 100 N normal loads. The initial Hertzian contact stresses and diameters (2a) were 1734 MPa and 235 μm under 50 N, and 2185 MPa and 296 μm under 100 N, respectively. Displacement amplitudes range from 10 to 100 μm (corresponding peak-to-peak strokes 20 to 200 μm) with a regular interval of 30 μm. Frequencies were varied from 200 to 20 Hz correspondingly to the displacement amplitudes, with an identical 8 mm/s linear speed for all cases which were repeated at least twice for each case. Fretting tests were run for 10, 30 and 90 min, which were equal to accumulated 4.8, 14.4 and 43.2 m sliding distances, respectively.

During the test, the normal force (P), tangential force (F_t) and displacements (D) were recorded simultaneously for every cycle as a function of time by a computer-based data acquisition system. The evolution of F_t-D curve was calculated by friction signal analysis (FSA) inbuilt software of SRV device. After the test, the specimens were ultrasonically cleaned again in ethanol bath for 20 minutes to get rid of loose wear debris and processed with compressed air blow.

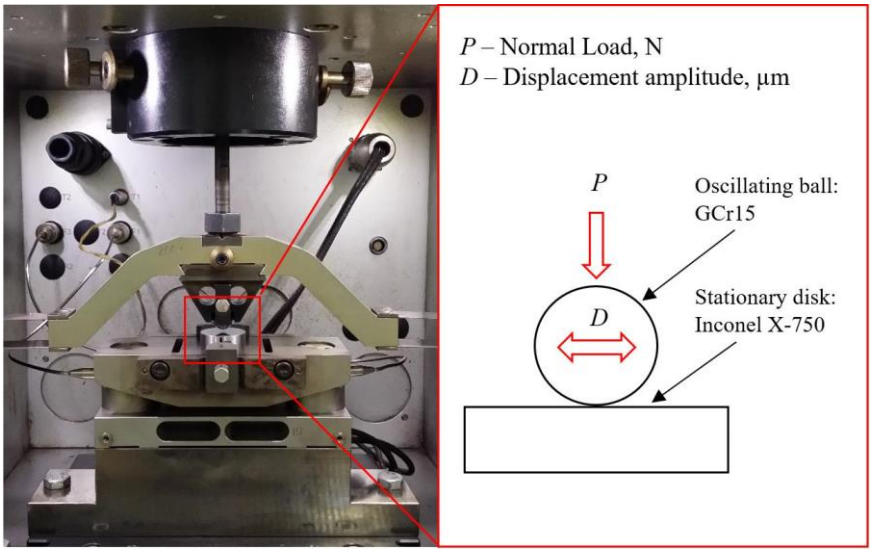

Fig. 2. SRV-4 fretting wear test apparatus and contact schematic of frictional pair.

After the fretting tests, Zygo Nexview (Lambda Photometrics Ltd, UK) 3D optical surface profiler was used to characterize the surface topography of the wear scar and to measure the wear volume below the original surface. This method adopts the principle of non-contact white light scanning interference, which is mainly used for the surface roughness of the optical and mechanical components. Worn surfaces were platinum (Pt) sputtered with 8.42 nm film thickness in the high vacuum coater system for the purpose of higher resolution morphology analysis. Then wear scar morphologies were investigated utilizing Tescan Lyra 3 (Czech Republic) scanning electron microscope (SEM) with the operating voltage of 15 kV inside the vacuum chamber (6e-2 Pa). Then the attachment system energy dispersive spectroscopy (EDS) is used to identify the elemental compositions of X-750 alloy in unworn and worn scar areas.

3. Results

3.1 Wear evolution

Optical images of wear scars formed on the flat specimen were illustrated in Fig. 3 for different amplitudes through time. As it is shown, the shape of wear scars was circular for all displacement amplitudes and grown in in size over time with negligible elongation in the sliding direction. The smallest wear scars were observed in the smallest amplitude of 10 μm, with deformed asperities in the stick area and slight damages in the slip annulus. Worn scar diameter and wear rate remains unchanged through time due to small oscillation. In the case of 40 μm, the shape of the wear scar was very close to the Mindlin`s definition of elastic model which the stick area in the contact center and micro-slip in the contact border became obvious due to PSR. The stick area was narrowed distinctly in 90 min and later replaced by full sliding in the interface for the larger displacement amplitudes, demonstrating from round to ellipsoidal shape with the maximum worn scar diameter of 1.75 mm and 27.3 μm depth at 100 μm amplitude.

Fig. 4 shows the wear volume information for the two loading conditions in respect of time and amplitude. Fig. 4 (a-row) plots the wear volume values as a function of time for displacement amplitudes under 50 N and 100 N. The wear progress was very slow in the lower displacement amplitude 10 μm for both loading cases, almost under 4.4×10^5 μm^3. Wear volume increased dramatically for 40 μm at 50 N, accumulating 8.4×10^5 μm^3 in 10 min and 33.5×10^5 μm^3 in 90 min. Under the same amplitude oscillation wear volumes for 100 N were 1.3-3.9 times smaller (6.5×10^5 μm^3 in 10 min and 8.4×10^5 μm^3 in 90 min) than 50 N. When the displacement amplitude exceeds 40 μm, gross slip takes place in both loading cases and the increase in wear volumes grows linearly. Wear volumes as a function of displacement amplitude for different test durations are given in Fig. 4 (b-row). Unlike larger loading state, wear volume slightly increased under 50 N in the lowest amplitude in a shortest period of fretting time as it was constant from 40 to 70 μm and again discreet increase was observed for the larger displacement amplitude. When fretting continues for a longer period of time, volume increase line becomes steep as the stroke length increases. Once normal load reaches to 100 N, small volumes of wear accumulated at 10 and 40 μm where PSR dominates. Fretting time has not influenced much on wear volume in this running condition. As the amplitude further increases, GSR starts and wear rate considerably grows over time, but eventually slows down above 100 μm.

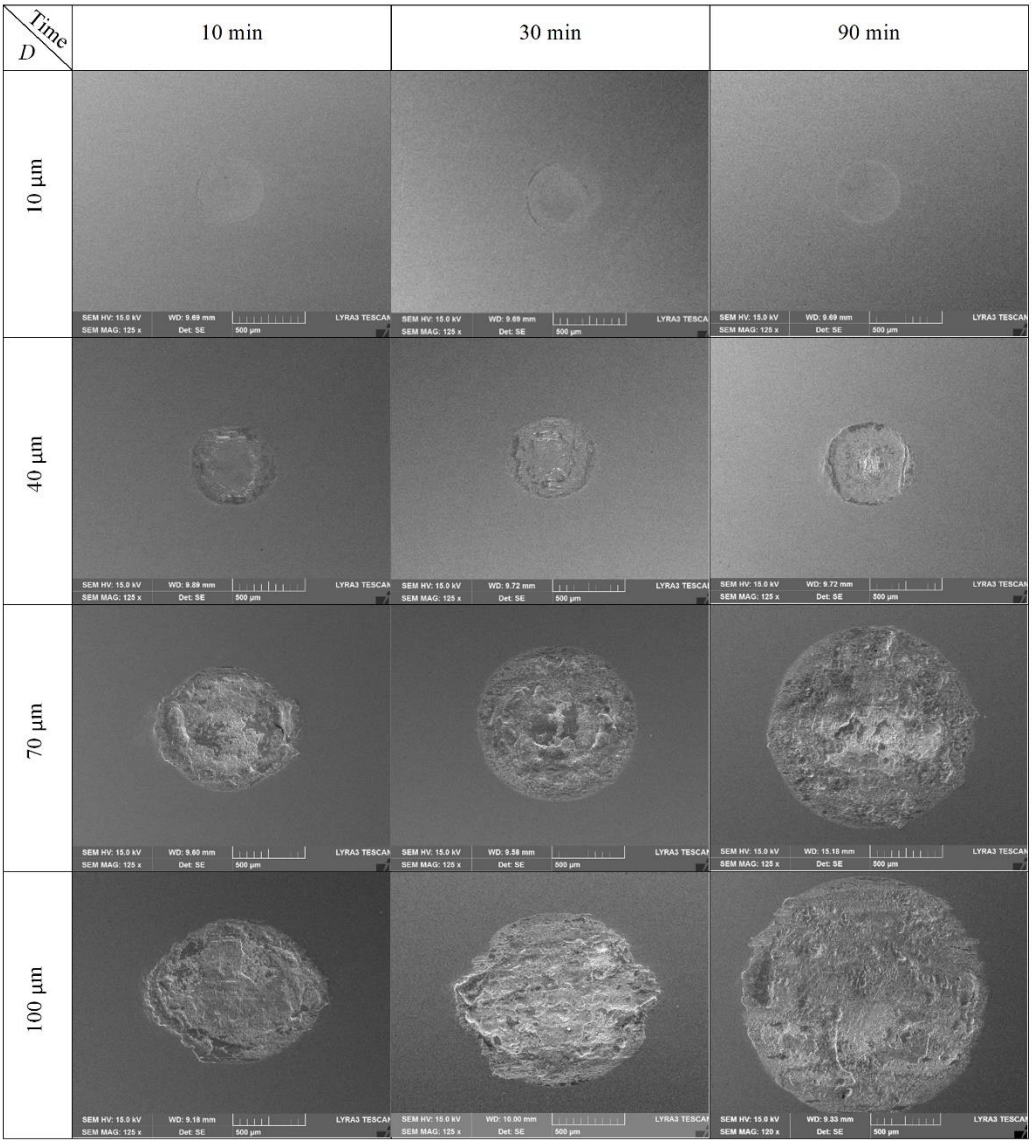

Fig. 3. SEM images of worn surfaces on lower specimens at displacement amplitudes of 10, 40, 70 and 100 µm (corresponding frequencies are 200, 50, 28.5 and 20 Hz, respectively) after 10, 30 and 90 min. Applied normal load is 100 N and fretting direction is horizontal.

Average wear volume plots are given for 50 N and 100 N in Fig. 4 (c-row) as a function of both time and displacement amplitude. Moreover, Fig. 5 gives some comparative scales of wear scars after 90 min fretting test in the case of 40 µm for two normal loading conditions. 3D-profile micrographs and cross-section profile perpendicular to the fretting direction show that wear scar of 50 N larger and deeper than 100 N and less wear debris produced under the greater loads until the

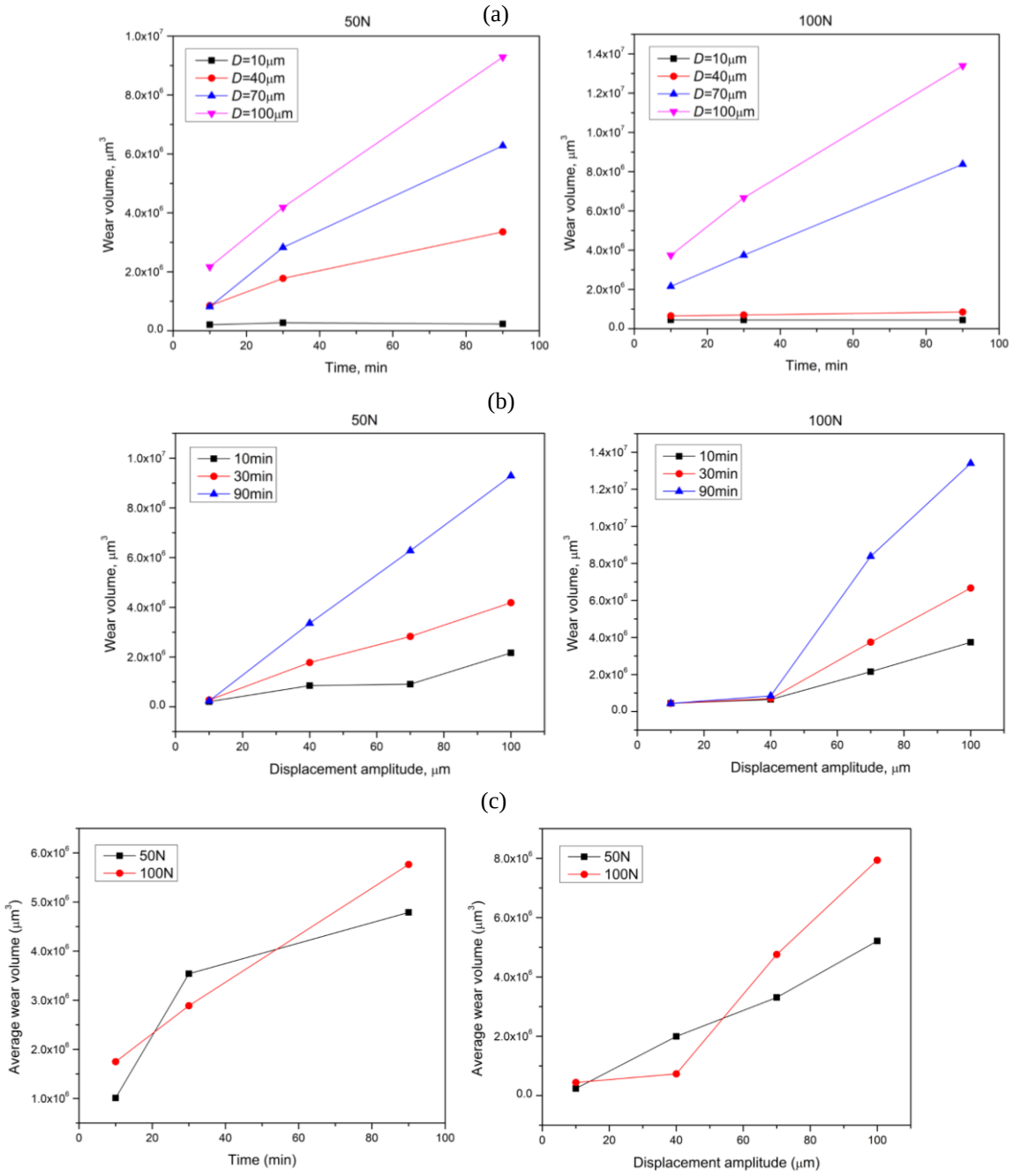

Fig. 4. Wear volume of lower specimen (a) as a function of time versus different displacement amplitudes; (b) as a function of displacement amplitude versus time and (c) average wear volume in respect of both time and displacement amplitude.

transition from PS to GS regime (≥40 μm) starts. In this point, the maximum scar depth of 50 N loading is about 17.8 μm which is 2.5 times deeper than 100 N (7.1 μm). Because of higher tangential force than normal force production in the case of lower loads, GSR takes over PSR in a smaller displacement amplitude compared to the higher loaded cases.

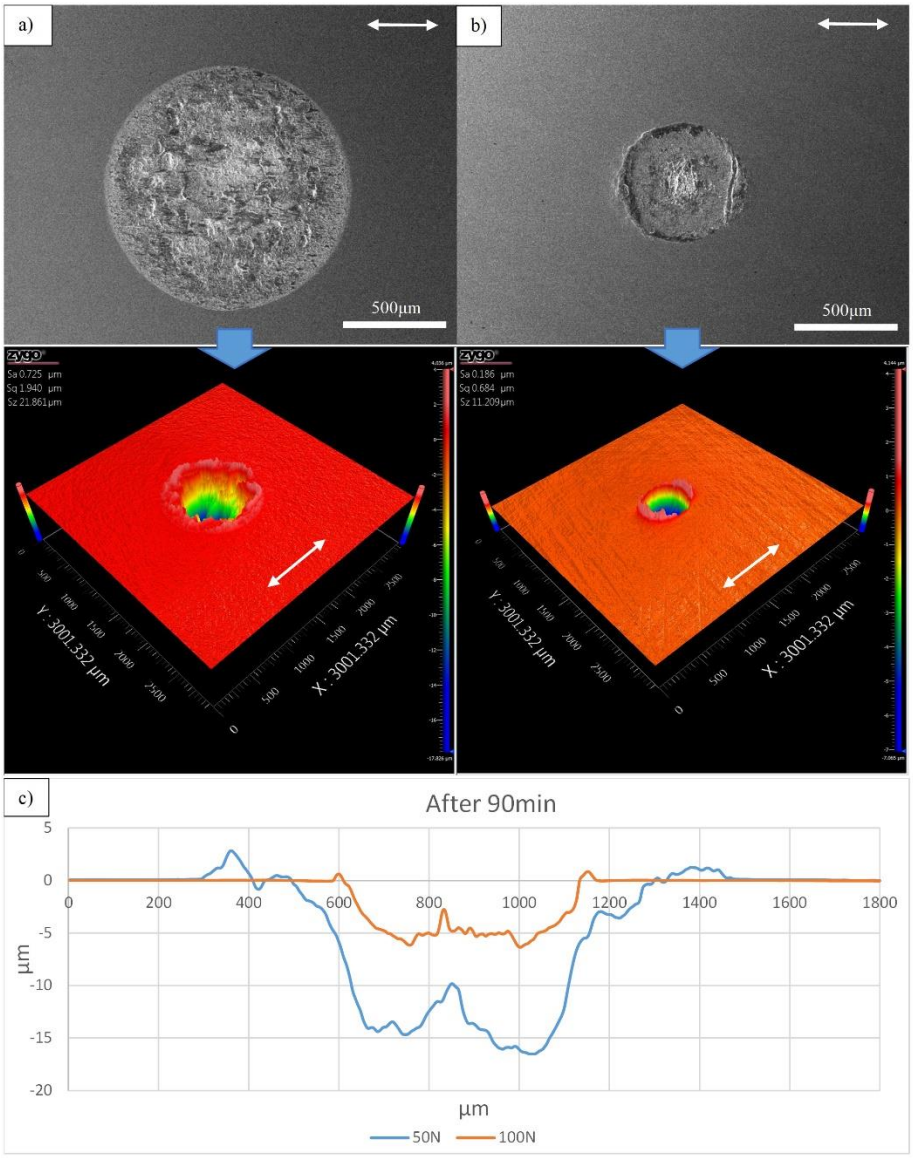

Fig. 5. Comparative SEM images under (a) 50 N and (b)100 N normal loads at 40 µm, and their 3D surface morphologies and (c) cross-section profiles perpendicular to fretting direction.

3.2 Frictional characteristics

Fig. 6 depicts the variations of coefficients of friction (CoF) versus time (for 0.5 h) for all displacement amplitudes under 50 N and 100 N normal loads. There is a rapid growth of CoF in the beginning within a few seconds to the maximal points and immediately stabilizes over time. The lowest CoF value (F_t/P = 2.5) was observed at 10 µm amplitude under 100 N, while friction force fluctuates around 0.41 at 50 N for the same sliding amplitude. In Fig. 6(b), CoF value in 40 µm jumped to the highest point and continued around at 0.82 for the rest of test. But for the higher displacement amplitudes (70 and 100 µm), gradual increase in CoF was observed till 300 s from the point of a jump (0.73), and then became steady-state at 0.92. Also, similar changes in CoF happened for higher amplitudes (including 40 µm) at 50 N and fluctuates about 0.89 till the test ends. Often drops in the friction curve were noticed in the largest amplitude values during fretting test because of debris entrapment and release between contacts as the oscillation became almost

reciprocating motion. The debris can alter the contact configuration from two-body to three-body contact, as a consequence of decrease and steady stage of CoF.

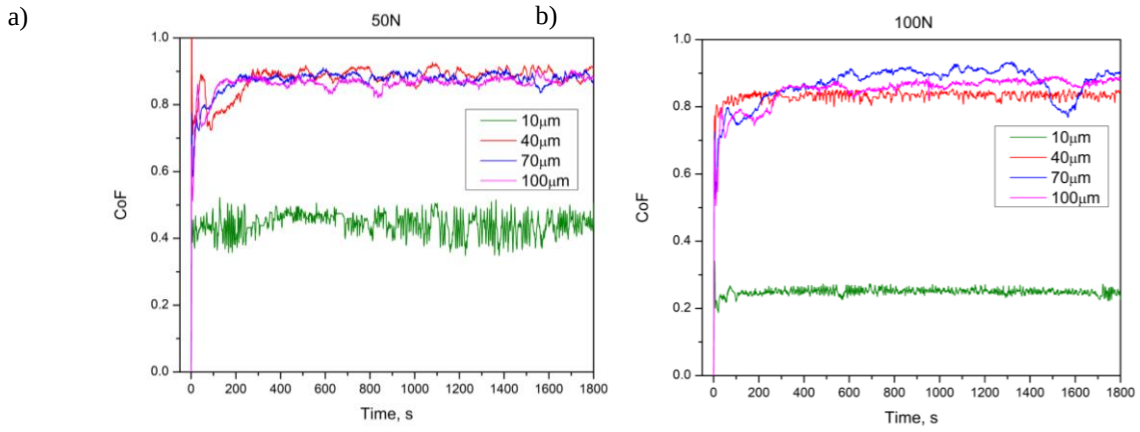

Fig. 6. Friction coefficients of GCr15/Inconel X-750 contact during 30 min.

In most of the theoretical and experimental fretting analysis, frictional logs (or fretting loops) of tangential force-displacement (F_t-D curve) relationships are used to describe the running characteristics of stick, partial slip and gross slip regimes. Fig. 7 shows the comparisons of fretting loops under different sliding regimes at 50 N and 100 N after 600 s of fretting test. In the stick regime (Fig.7a), linear or closed F_t-D relation is obtained for both loads and there is no sign of interfacial sliding in the contact interface. In the partial slip condition, sliding displacement and dissipation in the interface energy are relatively low as shown in Fig. 7(b). This elliptical F_t-D curve at 100 N is related to the transition from primary elastic to plastic shear form while the friction log has wider energy dissipation area but lower F_t value for 50 N. Fig. 7(c) and (d) attributed to gross slip regime where displacement amplitude and thus energy dissipation in the contact interface are greater. In this F_t-D shape close to parallelogram, full sliding can be observed through all contact area resulting in higher rate of wear damage and relative motions were predominantly accommodated by plastic deformation of counter surfaces during the entire fretting process. The shape of F_t-D curves remained almost same for the rest of the fretting tests. Details of material responses under such running conditions are discussed in the next chapter based on the results of SEM observations.

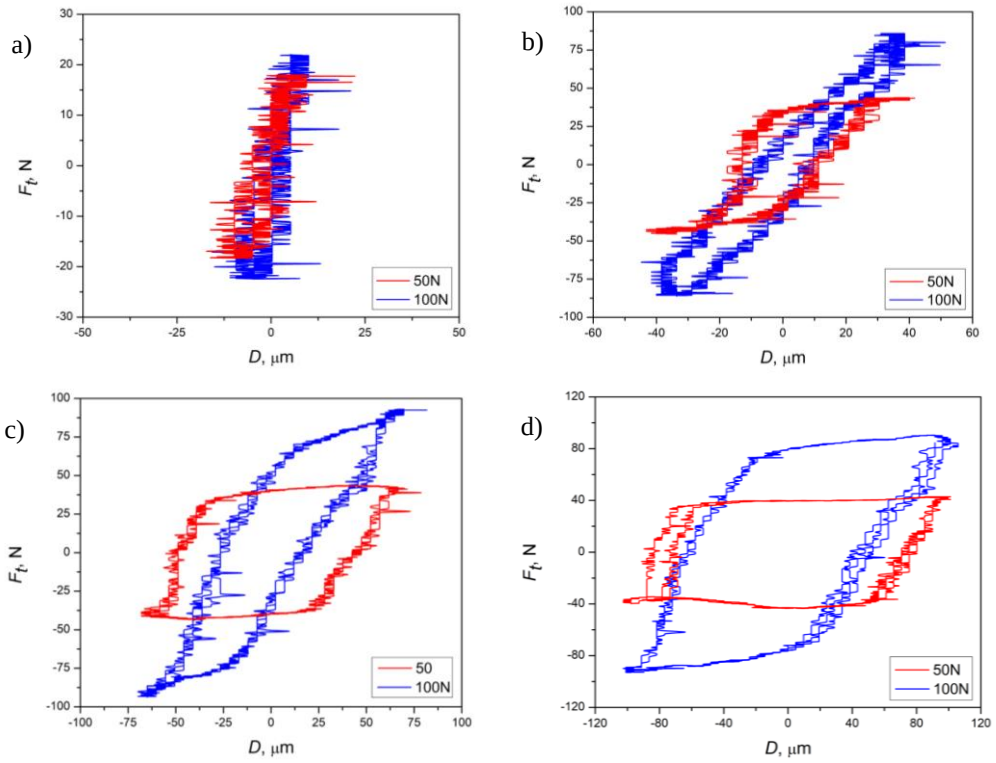

Fig. 7. Fretting loops of the contact assembly at (a) 10, (b) 40, (c) 70 and (d) 100 μm under different normal loads after 600 s.

3.3 Morphology analysis

Further investigations of wear scars on the Inconel X-750 alloy are carried out by observing SEM surface morphologies at different running conditions and corresponding material responses under these regimes are analyzed. Fig. 8 and Fig. 9 shows magnified SEM worn surface micrographs for PSR and GSR at 100 N. From Fig. 8(a) it is found that contact interfaces are stuck in the contact center where asperities are adhered and plastically sheared. Fretting scar with limited material loss was observed in a specimen at its periphery (Fig. 8b) because the slip is at the maximum in the periphery region compared to the center of the fretting motion. Wear mode is changed when displacement amplitude reached to 40 μm in Fig. 8(c) and (d) which is believed as a fatigue wear induced by cyclic loading. Stick area was slowly worn out during the fretting test due to overstressing and finally micro cracks perpendicular to fretting direction were detected after 90 min in the contact center but macro cracks are already formed earlier (after 30 min) in the slip annulus. This degradation mechanism can be attributed to mixed fretting regime (MFR) which is combined with stick and slip fretting phenomena and mainly responsible for crack nucleation and propagation [23]. Once cracks were developed, the stress cycles maintain high enough to nucleate cracks in the phase of GSR, subsequently removed by particle detachment.

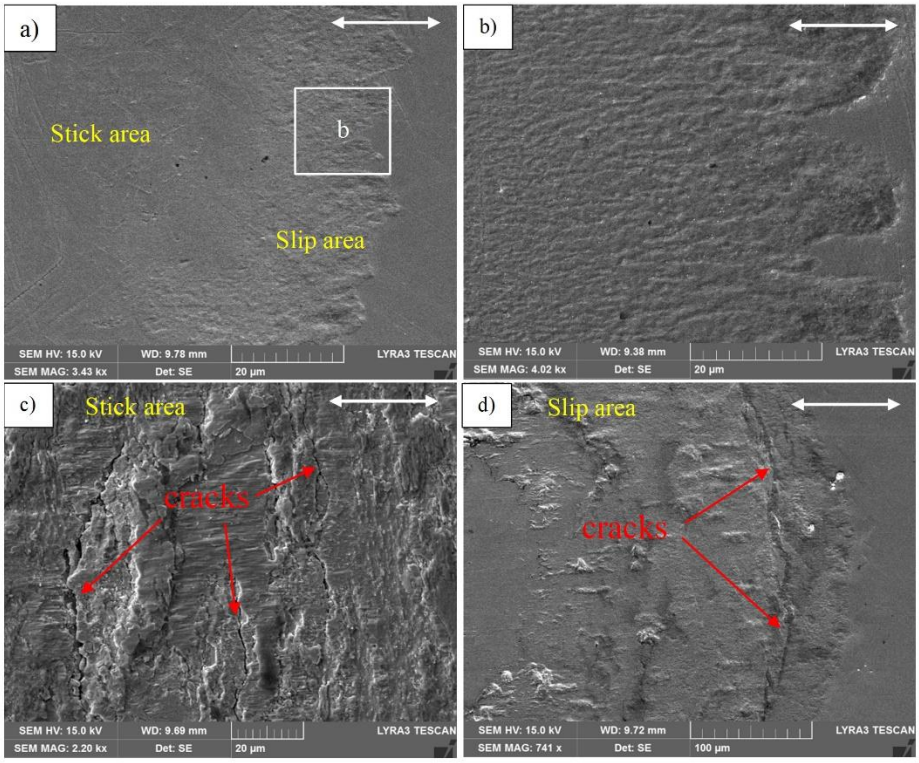

Fig. 8. SEM micrographs of wear scars and material responces under PSR: (a) Stick-slip regime at 10 µm and (b) magnified slip area; Partial slip at 40µm (c) magnified stick area after 90 min and (d) slip area after 30 min test. Applied normal load is 100 N and double arrow represents fretting direction.

In the transition point between PSR and GSR (displacement amplitude 70 µm) material removals were observed by abrasive and adhesive wear as shown in Fig. 9(a). Grooves parallel to fretting direction are formed due to larger relative motion and higher stresses between counter surfaces and thick layers were peeled off by adhesive wear, leaving wrinkles on the surface. On the other hand, cracks were started to spall into debris (magnified in Fig. 9b) and finally worn out by abrasive wear in the later stages of the test. With further increase of imposed amplitude, the extend of delamination and plastic flow developed gradually as shown in Fig. 9(c) and (d). Contact stresses were equally distributed to the relatively larger interfaces resulting in wider wear scar and the worn surface becomes rough owing to the plastic deformation and plowing effect. Some loose wear debris were also observed by the side of plastic flows. These obvious detachments at 100 N with greater displacement amplitude (70-100 µm) are relevant with wear modes of at 50 N and 40 µm sliding amplitude that worn scar morphology indicates the same wear mechanism of delamination by abrasion under GSR.

Fig. 10 shows the EDS analysis of unworn and worn surfaces on the flat specimen. It is found that oxygen content in the worn surface under 100 N is twice as higher (16 wt%) than that of worn surface at 50 N (8.2 wt%), which is believed that the worn area is covered with oxygen layer and increases with normal load. Oxidization process is strongly dependent on the humidity and temperature of the contact area which play crucial role and thus the consequences may become severe [24]. Reddish wear powder was extracted from the contact interface during the fretting process due to oxidized metallic particles. Oxide film is formed in the contact interface and broken under the sliding action, so the fresh surface becomes chemically active and again newly oxidize. This process accelerates the corrosion of worn surface and this tendency is much higher at higher normal loads [25]. In addition, iron (Fe) content also increased in the worn surface, mainly due to material transfer effect by GCr15 steel ball in the fretting process.

4. Discussion

According to the experimental results under the given conditions, the fretting wear of Inconel X-750 alloy strongly depends on the test duration, oscillation amplitudes and exerted normal loads. Time dependence of fretting wear has been observed in several bearing materials; however, the real nature of dependence was also the mechanical properties of the contacting materials and test conditions [12,16,26]. Moreover, it is known from the previous studies that fretting wear in air is also determined by the contact configuration, oxidation process and wear debris between contact surfaces. It can be considered that friction is a function of third-body rheology, while wear is a function of third-body flow such as source

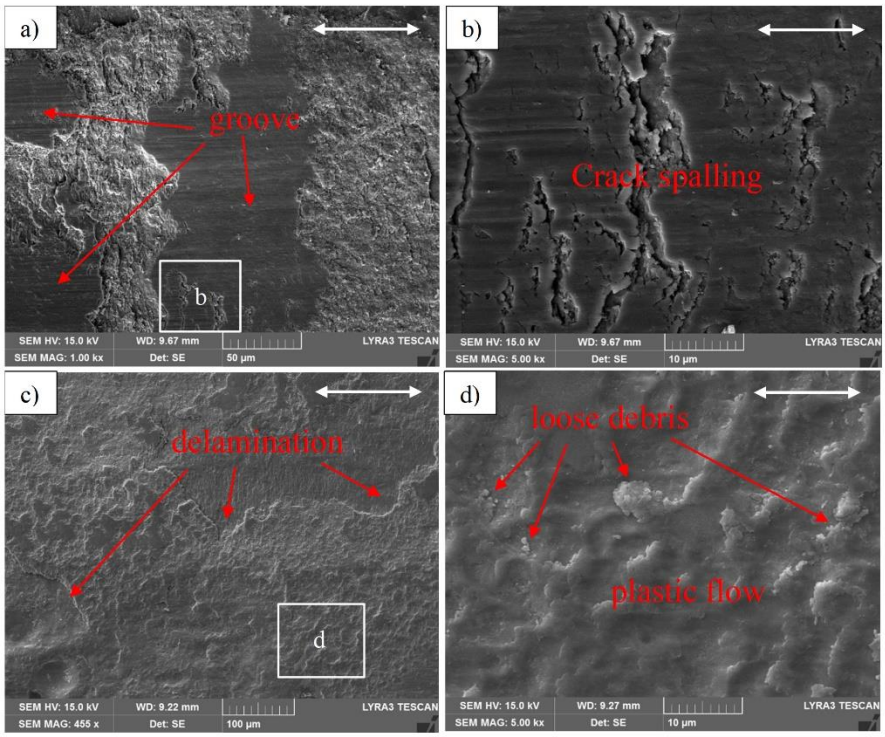

Fig. 9. SEM micrographs of wear scars and material responces under GSR: (a) Onset of GSR regime at 70 µm and (b) magnified area at (a); (c) GSR at 100 µm and (d) magnified area at (c). Applied normal load is 100 N and double arrow represents fretting direction.

flow, ejection flow and wear flow [27,28]. More oxide debris will be generated as displacement amplitude increases during the fretting and temporarily trapped for some time in the contact which impacts on the friction and wear process in dry condition [16,29]. Therefore, wear damage has grown linearly with stroke length in Fig. 4(a) and (b), whereas the slight wear rate observed at 10 and 40 µm under 100 N, following rapid wear damage at 70 and 100 µm. Wear rate is believed to be nearly constant when the sliding regime switches to the reciprocating motion [13].

It should be noted that at 40 µm, the sliding regimes were gross slip and partial slip for 50 N and 100 N, respectively, and the surface degradation differentiated prominently as shown in Fig. 5. The initial increase in the friction coefficient in Fig. 6 is due to the elimination of *"surface complexes"* (or oxide and contaminant layer) and increase in the first-body interactions, accompanied by work-hardening of the surface structure. On the other hand, the fluctuations on the CoF curve at higher oscillating amplitudes are attributed to the actual changes of the contact interface linked to the debris formation and their ejection from the contact zone [10,15].

Based on the existing literatures, the total area of the friction loops in Fig. 1(a) represents the dissipated energy by friction during each cycle [4,5,23]. Corresponding F_t-D curves in Fig. 7 are shaped as a linear, elliptical and finally converted to parallelogram, where partial slip, mixed regime and gross slip regimes took place, respectively. Depending on the sliding regimes, consequential damages have been observed by SEM surface morphology which usually combined with adhesive wear, abrasive wear, oxidative wear and thick debris delamination.

Crack formation and wear debris production are the two challenging degradation processes during fretting and the possibility for each to prevail will depend on the contact pressure and the relative oscillating amplitude as shown in Fig. 1(b). Under the PSR and MFR, asperity adhesion, crack nucleation and propagations were induced by fretting fatigue as shown in Fig. 8, while debris formation and material removal were generalized for GSR. The sliding regimes

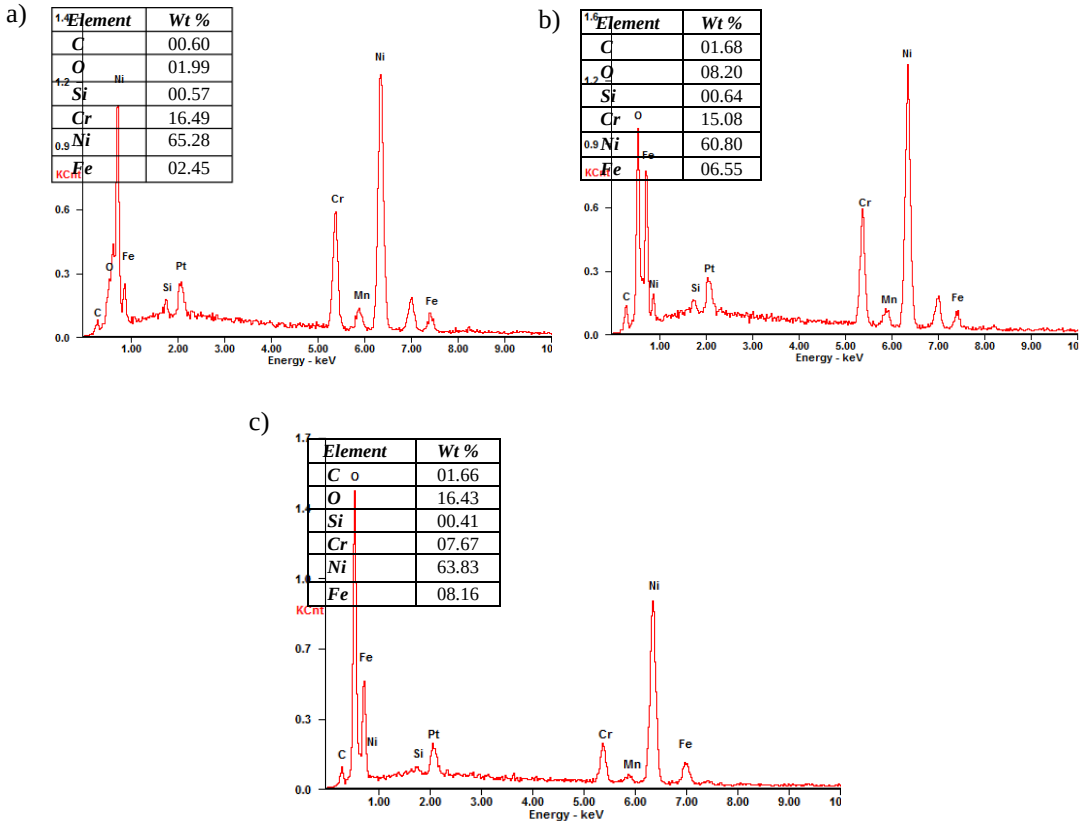

Fig. 10. Energy dispersive spectra (EDS) of (a) unworn surface, worn surfaces at (b) 50 N and (c) 100 N during GSR after 90 min.

are varied with the normal load at the same imposed amplitude [4]. Early crack initiation is regarded as the most crucial aspect for determining service life. For smaller amplitudes the influence of fretting can be ignored and crack behavior is associated with the fatigue mechanism. For higher displacements, fretting was characterized as a wear behavior. MFR is mainly dominated by the fretting conditions, such as the relative slip and normal load. Crack nucleation can be decelerated under the external cyclic stress correlated with relative oscillation, or the service life of Alloy X-750 can be prolonged by adjusting particular fretting conditions, i.e., normal load.

In Fig. 8(b) and (c) cracks are initiated after a certain number of repetitive cycles owing to high contact stress. The progressive elimination of the stick and slip domain with the time duration and higher displacement amplitude will accumulate debris particles which results in a three-body

abrasion with grooves parallel to the fretting direction as shown in Fig. 9(a). The cracks are spalled thus removed leaving large chipping pits behind on the contact surface (Fig. 9b). The continuation of movement between the counter surfaces then leads to a surface degradation resulting in a delamination wear and plastic flow as given in Fig. 9(c) and (d). In addition, it was clearly observed in Fig. 10 that the oxygen content was excessive on the worn surfaces, and tends to accumulate thick concentration with the increase of the displacement amplitude and normal load. This can be attributed to the more mechanical energy being transferred to the thermal energy [30].

5. Conclusion

In this study, the effects of the displacement amplitudes, normal loads and time on the fretting behaviors of Inconel X-750 alloy were studied in dry condition. Worn surfaces were analyzed by 3D optical profiler and SEM morphologies. The results can be summarized as following:

1. Displacement amplitude was an important factor in the process of the friction and wear damage where a significant growth was detected on both CoF and wear volume with the increase of amplitude. This is because the sliding regime was gradually transforming from partial slip to full slip. Sliding regime in the case of displacement amplitude ≤ 40 μm, PSR was dominant. Wear mechanisms are combined with the local adhesion in the stick zone, slight fretting degradation in the slip zone and cracking by overstressing cyclic loads. As the process continues, the condition changes to GSR for larger amplitudes between contact surfaces and, as a result, oxidized debris is generated.
2. Imposed normal load determines the wear mode of the materials. When normal load is low, the tangential force dominates over the static CoF even in a smaller displacement amplitudes and wear mode is correlated with the abrasive wear, however, crack propagation by spalling and wear delamination were dominated under the greater normal loads.
3. Wear damage was found to be very progressive over time during the fretting test for higher displacements while size of the wear scar was unchanged over time under the PSR at higher normal loads. Thus, the influence of the test duration in PSR was found to be less consistent. Usually, wear is rapid for the number of cycles on a surface damage, nevertheless, in GSR, heavily surface degradations occurred after a few minutes. Once the third-body particles accommodate in the interface, time dependence on the wear volume becomes irrelevant.

Acknowledgements

This work is supported by Aeronautical Science Fund of China (Grant No. 20164058002) and the National Natural Science Foundation of China (Grant No.51735006). The first author would like to thank the State Key Laboratory of Tribology at Tsinghua University for its huge contribution on the experimental works, and kind guidance of Prof. Zixi Wang.

References

[1]. Zhou Z.R., Fayeulle S. and Vincent L. Cracking behavior of various aluminum alloys during fretting wear. Wear 1992, 155, 317-330.

[2]. Vincent L, Berthier Y, Dobourg M C, and Godet M. Mechanics and Materials in Fretting. Wear, 153, 1992, 135-148.

[3]. Mindlin R D. Compliance of elastic bodies in contact. ASME J. Appl. Mech. 1949; 16:259-68.

[4]. Zhou Z R, Vincent L. Mixed fretting regime. Wear 181-183 (1995) 531-536

[5]. Fouvry S, Kapsa Ph, Hassan Z, Vincent L. Wear analysis in fretting of hard coatings through a dissipated energy concept. Wear 203-204 (1997) 393-493.

[6]. Gwidon W S. Wear-Materials, Mechanisms and Practice. John Wiley and Sons, Ltd. 2005.

[7]. Stachowiak G B, Stachowiak G W. Fretting wear and friction behavior of engineering ceramics. Wear 190 (1995) 212-218.

[8]. Ohmae N, Tsukizoe T. The effect of slip amplitude on fretting. Wear 27 (1974) 281-294.

[9]. Toth L. The investigation of the steady state of steel fretting. Wear 20 (1972) 277–283.

[10]. Lewis M J, Didsbury P B. The rubbing fretting behaviour of mild steel in air at room temperature: the effects of load, frequency, slip amplitude and test duration. Treatise on Material Science and Technology, Vol. 136, Academic Press, New York, 1979.

[11]. Vingsbo O, Soderberg S. On fretting maps, Wear 126 (1988) 131-147.

[12]. Vizintin J, Kalin M, Novak S, Drazic G, Ives L K, Peterson M B. Effect of slip amplitude on the fretting wear of silicon nitride against silicon nitride. Wear192(1996) 11-20.

[13]. Baker R F, Olver A V. Direct observation of fretting wear of steel. Wear 203-204 (1997) 425-433.

[14]. De Baets P, Strijckmans K, van Peteghem A P. Characterization of the fretting wear of unlubricated steel surfaces based on the comparison of wear results obtained by different methods. Wear 208 (1997) 169-176.

[15]. Chen G X, Zhou Z R. Study on transition between fretting and reciprocating sliding wear. Wear 250 (2001) 665-672

[16]. Li J, Lu Y H. Effects of displacement amplitude on fretting wear behaviors and mechanism of Inconel 600 alloy. Wear 304 (2013) 223-230.

[17]. Long X, ZiHao W, Jie L, Yonghao L, Tetsuo S. Microstructural characterization of subsurface caused by fretting wear of Inconel 690TT alloy. Materials Characterization 115 (2016) 32-38.

[18]. Qiufeng W, Yunxia W, Hongling W, Na F, Fengyuan Y. Experimental investigation on tribological behavior of several polymer materials under reciprocating sliding and fretting wear conditions. Tribology International 104 (2016) 73-82.

[19]. Liu E, Blanpain B, Celis J P. Fretting friction and wear of polycrystalline diamond coatings. Diamond and Related Materials 5 (1996) 649-653.

[20]. Dongxing D, Daoxin L, Zuoyan Y, Xiaohua Zh, Fanqiao L, Ziqi Z, Lei Y. Fretting wear and fretting fatigue behaviors of diamond-like carbon and graphite-like carbon films deposited on Ti-6Al-4V alloy. Applied Surface Science 313 (2014) 462-469.

[21]. Wenbo D, Yanhua S, Chunhua D, Lie Y. Structural stiffness of X-750 alloy bump foil strips for compliant foil bearings with different heat treatments. Journal of Tribology, Vol. 138 / 031702-1. 2016.

[22]. Jon S L, Alejandro C V, Ilmar F S. Numerical and experimental investigation of bump foil mechanical behavior. Tribology International 74 (2014) 46-56.

[23]. Zhou Z R, Nakazawa K, Zhu M H, Maruyama N, Kapsa Ph, Vincent L. Progress in fretting maps. Tribology International 39 (2006) 1068-1073.

[24]. Yu J, Cai Z B, Zhu M H, Qu S X, Zhou Z R. Study on torsional fretting behavior of UHMWPE. Applied Surface Science 2008; 255 (2):616-8.
[25]. Zhu M H, Zhou Z R. On the mechanisms of various fretting wear modes. Tribology International 44 (2011) 1378-1388.
[26]. Long X, Huijuan L, Junling H, Yonghao L, Tetsuo S. Damage mechanism of Alloy 690TT mated with Type 304 stainless steel during fretting wear in partial slip regime. Materials Characterization 132 (2017) 284-292.
[27]. Berthier Y. Background on Friction and Wear. Handbook of Materials Behavior Models. Chapter 8, Lemaître Academic Press, 2001, pp. 676-699, ISBN 0124433413.
[28]. Iordanoff I, Seve B and Berthier Y. Solid Third Body Analysis Using a Discreet Approach: Influence of Adhesion and Particle Size on Macroscopic Properties. ASME Journal of Tribology, 124, 2002, 530-538.
[29]. Jie L,Yonghao L, Haoyang Z, Long X. Effect of grain size and hardness on fretting wear behavior of Inconel 600 alloys. Tribology International 81 (2015) 215-222.
[30]. Xianglong G, Ping L, Lichen T, Jiamei W, Lefu Zh. Effects of sliding amplitude and normal load on the fretting wear behavior of alloy 690 tube exposed to high temperature water. Tribology International 116 (2017) 155-163.